10.24425/acs.2020.135848

*Archives of Control Sciences*
*Volume* 30(LXVI), 2020
*No.* 4*, pages 701–719*

# Tuning rules for industrial use of the second-order Reduced Active Disturbance Rejection Controller

P. NOWAK, J. CZECZOT and P. GRELEWICZ

In the paper, problem of proper tuning of second-order Reduced Active Disturbance Rejection Controller (RADRC2) is considered in application for industrial processes with significant (but not dominant) delay time. For First-Order plus Delay Time (FOPDT) and Second-Order plus Delay Time (SOPDT) processes, tuning rules are derived to provide minimal Integral Absolute Error (IAE) assuming robustness defined by gain and phase margins. Derivation was made using optimization procedure based on D-partition method. The paper also shows results of comprehensive simulation validation based on examplary benchmark processes of more complex dynamics as well as final practical validation. Comparison with PID controller shows that RADRC2 tuned by the proposed rules can be practical alternative for industrial control applications.

**Key words:** reduced-order ADRC, tuning, practical validation, industrial application

## 1. Introduction

Since its first English introduction [5], Active Disturbance Rejection Controller (ADRC) received huge attention from both academia and industry as the concept that promises effective control without detailed process modeling. Shortly speaking, it is based on unified representation of process dynamics [9, 22]. This dynamic jointly with external disturbances are compensated by application of Extended State Observer (ESO). Then, in ADRC control law, process dynamics can be simplified to a cascade of integrators.



All Authors are with Silesian University of Technology, Department of Automatic Control and Robotics, ul. Akademicka 16, 44-100 Gliwice, Poland. J. Czeczot is the corresponding author, E-mail: jacek.czeczot@polsl.pl.

Paweł Nowak and Jacek Czeczot were financed by the grant from the Silesian University of Technology – subsidy for maintaining and developing the research potential in 2020. Patryk Grelewicz was financed by the European Union through the European Social Fund (grant POWR.03.02.00-00-I029).

Rceived 19.03.2020. Revised 10.11.2020.

Apart from a huge number of applications for drive control systems, ADRC becomes more and more popular in process automation as a potential alternative for conventional PID controllers [10, 11, 16]. At the same time, popularity of reduced-order ADRC (RADRC) [8] is also growing due to easier implementation and to reduction of phase lag comparing to conventional ADRC approach [19].

From a practical point of view, further increase in popularity of both algorithms (ADRC and RADRC) depends on meeting certain requirements. The first is a simple implementation in the form of function blocks in Programmable Logic Controllers (PLC). For this case, some solutions can be found in works [7, 12]. The second even more critical requirement is to develop relatively simple and effective tuning methods. Several tuning methods can be found for ADRC [3, 16, 21]. By contrast, according to the best authors' knowledge, such a tuning method was reported only for the first order RADRC (RADRC1) [13].

This paper concentrates on further development of industrial applicability of RADRC approach. Namely, derivation of tuning method for the second-order RADRC (RADRC2) is considered. Motivation for this research results from the fact that potentially, in some cases RADRC2 is able to provide better control performance comparing to RADRC1 but its robust and reliable tuning is still a bottleneck.

There are two potential process approximations that can be considered as a basis for tuning of RADRC2: one is FOPDT and the other is SOPDT model. Both of them can be derived using process step response. In this paper, both approximations are considered and for both of them, robust tuning rules are developed by optimization method and assuming certain gain and phase margins. Then, the suggested tuning rules are validated by simulation based on the selected benchmark processes of different complex dynamics. Practical validation for the laboratory pneumatic setup completes the paper and results are summarized in conclusions.

The major novelty of this paper results from the following contributions:

- suggesting the approach for RADRC2 tuning using D-partition method,
- derivation of four RADRC2 tuning rules including rules based on SOPDT model,
- simulation verification of the proposed methods for complex benchmark processes,
- practical verification based on the pneumatic laboratory setup.

## 2. Problem statement and motivation

This study concentrates on RADRC2 control of lag-dominated processes with significant dead time $T_0$ and more complex stable dynamics. For controller design, it is assumed that these processes can be approximately described by the simplified model:

$$\ddot{Y}(t) = F\left(\dot{Y}(t), Y(t), d(t), u(t - T_0)\right) + b_0 u(t), \tag{1}$$

where $Y$ is a measured controlled variable, $u$ is a manipulating variable, $d$ represents disturbances, $b_0$ is a scaling factor that potentially can be used as a tuning parameter [20] and $F(\,)$ is an unknown nonlinear function called a total disturbance and including process nonlinearities and potential modeling inaccuracies. Readers should note presence of delay time $T_0$ in Eq. (1).

In general, ADRC methodology applies unified extended state observer (ESO) to estimate the total disturbance $F(\,)$, controlled variable $Y$ and its consecutive time derivatives to provide compensation for higher-order dynamics. In process automation, when $Y$ is measured, reduced-order ESO (RESO) can be applied [8]. For the considered case of second-order process model (1), RESO has the following form:

$$\begin{aligned}
\dot{z}_2' &= -2\omega_o z_2' + z_3' - 3\omega_o Y + b_0 u,\\
\dot{z}_3' &= -\omega_o^2 z_2' - 2\omega_o^3 Y,\\
z_2 &= z_2' + 2\omega_o Y,\\
z_3 &= z_3' + \omega_o^2 Y,
\end{aligned} \tag{2}$$

where $z_2$ and $z_3$ respectively estimate $\dot{Y}$ and $F(\,)$. Auxiliary variables $z_2'$ and $z_3'$ are introduced to avoid numerical computation of $\dot{Y}$. Tuning of RESO (2) is made by proper adjusting the observer bandwidth $\omega_o$ [6]. Assuming that $z_3 \approx F(\,)$ and using a simple control law in the form $u = (u_0 - z_3)/b_0$, the complex process (1) can be reduced to a simple double integral form. Then, this type of process can be easily controlled by conventional PD controller, so the final form of RADRC2 control law is:

$$u = \frac{\omega_c^2\,(SP - Y) - 2\omega_c z_2 - z_3}{b_0}, \tag{3}$$

where $SP$ is the set-point and $\omega_c$ is the RADRC2 tuning parameter (controller bandwidth [6]). In general, RADRC2 has three tuning parameters $\omega_o$ (2) $\omega_c$ (3) and $b_0$ (1). Adjustment of their values is discussed in the next section.

## 3. D-partition method for RADRC2 tuning

In this paper, derivation of tuning rules for RADRC2 is based on application of D-partition method for determining correlation between parameters of closed-loop characteristic equation and stability region on controller parameter plane [1, 14]. This concept was successfully applied for deriving tuning rules for RADRC1 based on process FOPDT approximation and readers are referred to [13] for more details. In this paper, it is shown how this concept was adapted for a much more complex case of RADRC2 control of industrial processes. Only the most important stages and the most significant differences are described.

When a process assumed as FOPDT or SOPDT is to be controlled by RADRC2, closed-loop system must be completed with virtual gain-phase margin tester to determine gain or phase margin boundary [18, 20]. The gain-phase margin tester is a virtual block defined as $A\,e^{-j\varphi}$ where $A$ and $\varphi$ are real values representing assumed virtual gain and phase, respectively. Then, after applying Laplace transform to Eqs. (2) and (3), this system can be represented as it is shown in Fig. 1. Note that its complexity exceeds similar cases with PID controller and with ADRC1, which promises a potential improvement in control performance.

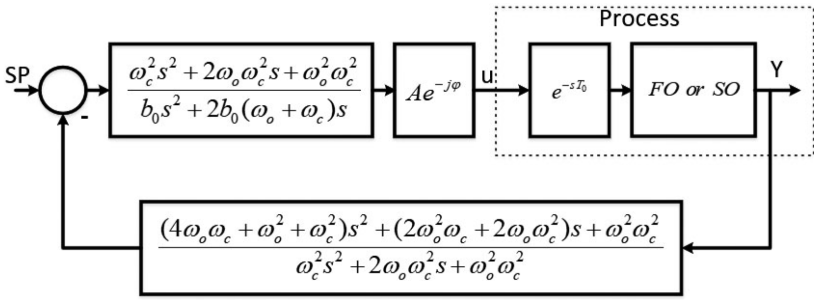


Figure 1: Representation of the closed-loop system with RADRC2 and gain-margin tester

After deriving open-loop transfer function of the control system, characteristic equation $\chi(s) = 0$ can be determined. Then, after assuming $b_0 = \text{const}$ and substituting $s = j\omega$, $e^{-j(\omega T_0+\varphi)} = \cos(\omega T_0 + \varphi) - j\sin(\omega T_0 + \varphi)$, location of roots of characteristic equation depends only on the values of RADRC2 tuning parameters $\omega_c$, $\omega_o$, on FOPDT/SOPDT process parameters and on assumed virtual gain $A$ and phase $\varphi$ margins. $\chi(s) = 0$ has three possible solutions called D-boundaries, which correspond to $\omega = 0$ (real roots boundary), $0 < \omega < \infty$ and $\omega \to \infty$ (complex roots boundary). Then, for $\omega = 0$, two intuitive boundaries $\omega_c = 0$, $\omega_o = 0$ are derived. At the same time, the boundary for $0 < \omega < \infty$ can be decomposed into its real and imaginary parts forming the following set of highly nonlinear stability equations:

$$\begin{aligned}
\operatorname{Re}\{\chi(s)\} &= A_1\omega_c + B_1\omega_o + C_1\omega_c^2 + D_1\omega_o^2 + E_1\omega_c\omega_o + \\
&\quad + F_1\omega_c^2\omega_o + G_1\omega_c\omega_o^2 + H_1\omega_c^2\omega_o^2 + I_1 = 0, \\
\operatorname{Im}\{\chi(s)\} &= A_2\omega_c + B_2\omega_o + C_2\omega_c^2 + D_2\omega_o^2 + E_2\omega_c\omega_o + \\
&\quad + F_2\omega_c^2\omega_o + G_2\omega_c\omega_o^2 + H_2\omega_c^2\omega_o^2 + I_2 = 0,
\end{aligned} \tag{4}$$

where $A_1, A_2, B_1, B_2, C_1, C_2, D_1, D_2, E_1, E_2, F_1, F_2, G_1, G_2, H_1, H_2, I_1, I_2$ are the real coefficients depending on FOPDT/SOPDT process parameters, on assumed gain-phase margins $A$, $\varphi$, on RADRC2 tuning parameter $b_0$ and on frequency $\omega$. By assuming required gain $A$ and phase $\varphi$ margins, for a certain process, one can determine gain (GM) and phase (PM) margin boundaries that determine GM/PM margin region at $\omega_c - \omega_o$ parameter plane [20]. When the tunings $\omega_c$, $\omega_o$ are located within this region, closed-loop system preserves required or higher gain and phase margins. However, potentially there is an infinite number of tunings location that meet the desired GM/PM requirements but for all of them, control performance can be different. Thus, optimization procedure must be applied to determine the tunings $\omega_c$, $\omega_o$ that not only preserve GM/PM margins but also minimizes assumed control performance index. Readers should note that this procedure should also consider the influence of $b_0$ because as it was said before, it is very important RADRC2 tuning parameter.

In this work, it is assumed that RADRC2-based closed-loop system shown in Fig. 1 should minimize Integral Absolute Error (IAE) for load disturbance rejection, defined as:

$$Q\left(b_0, \omega_c, \omega_o\right) = \int\limits_0^{T_{\max}} |SP - Y|\, \mathrm{d}t. \tag{5}$$

Then, the constrained optimization problem is defined as:

$$\begin{aligned} &\underset{b_0,\omega_c,\omega_o\in\mathcal{R}^+}{\text{minimize}}\ Q \\ &\text{subject to GM} \geqslant \text{GM}_{\text{bound}} \ \text{ and} \\ &\qquad\qquad \text{PM} \geqslant \text{PM}_{\text{bound}}\,, \end{aligned} \tag{6}$$

where $\text{GM}_{\text{bound}}$ and $\text{PM}_{\text{bound}}$ denote defined GM/PM margin boundaries. This problem is convex but still complex so it needs to be solved numerically, as it is partially described in [13]. This procedure allows for adjusting optimal settings that ensure assumed amplitude and phase margins. However, it has very high complexity. From a practical point of view, direct form of the tuning rules that are ready to be used and based on the chosen approximation of process dynamics is preferred. This form is derived in the next section.

## 4. RADRC2 tunings rules derivation

First, let us assume that the process has FOPDT dynamics and it is to be controlled by RADRC2. It is assumed to concentrate on lag-dominated processes with relative delay time $L = T_0/T$ limited to $0 < L \leqslant 1$, where $T_0$ and $T$ are respectively delay time and time constant of FOPDT process. Fig. 2 shows examplary solution of the problem (6) for assumed GM = 2.5 and PM = 60°, obtained for FOPDT processes of different $L$ value. The solution was numerically computed for FOPDT processes of unitary gain and of different $L$ and these results are denoted by '*'. Solid lines represent approximating formulas describing tuning rule – in this case, the rule A1 given by Eq. (7). In a very similar way, the tuning rule A2 was derived for GM = 2 and PM = 45° and it is given by Eq. (8). Both tuning rules are normalized with respect to process gain $k$ and its time constant $T$.

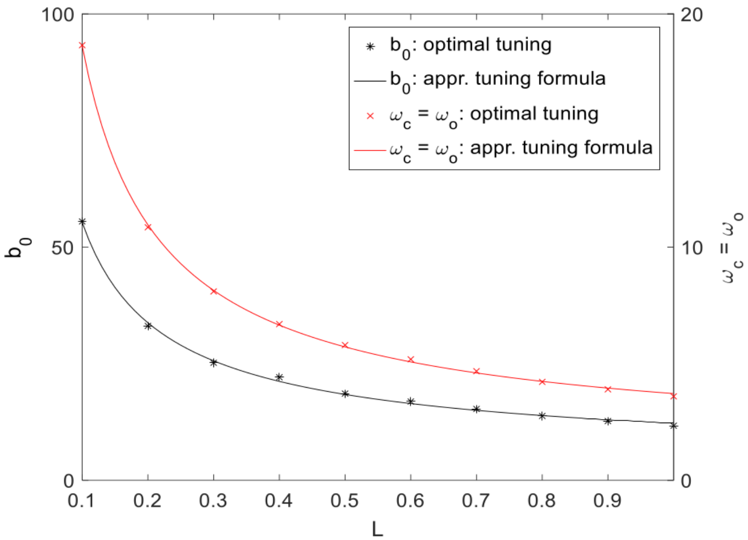


Figure 2: Optimal RADRC2 tunings vs. FOPDT relative delay time $L$, for GM = 2.5, PM = 60°

A1: RADRC2 tuning rule for FOPDT process, GM = 2.5, PM = 60°, disturbance rejection

$$b_0 = \left(8.38L^{-0.62} + 5.25\right)\frac{k}{T^2},$$
$$\omega_c = \omega_o = \left(2.14L^{-0.7} + 1.32\right)\frac{1}{T}. \tag{7}$$

A2: RADRC2 tuning rule for FOPDT process, GM = 2, PM = 45°, disturbance rejection

$$b_0 = \left(8.63L^{-0.78} + 3.62\right)\frac{k}{T^2},$$
$$\omega_c = \omega_o = \left(2.55L^{-083} + 1.17\right)\frac{1}{T}. \tag{8}$$

Methodology described in Section 3 allows also for deriving tuning rules for RADRC2 applied for control of processes that have SOPDT dynamics. For this purpose, minimization of (5), (6) was computed for the control system shown in Fig. 1 with SOPDT processes with unitary gain, two time constants $T_1 \geqslant T_2$ and time delay $T_0$. Fig. 3 shows results for assumed GM = 2.5 and PM = 60°, for SOPDT processes of different ratios $L_1 = T_0/T_1$ and $L_2 = T_2/T_1$ characterizing their dynamics. It is assumed to concentrate on processes with the limitations $0 < L_1 \leqslant 1$ and $0.4 \leqslant L_2 \leqslant 1$. The second limitation results from the fact that for such processes significantly dominated by time constant $T_1$ ($L_2 < 0.4$), a very similar control performance can be obtained when one of tuning rules A1–A2 is applied based on the FOPDT process approximation.

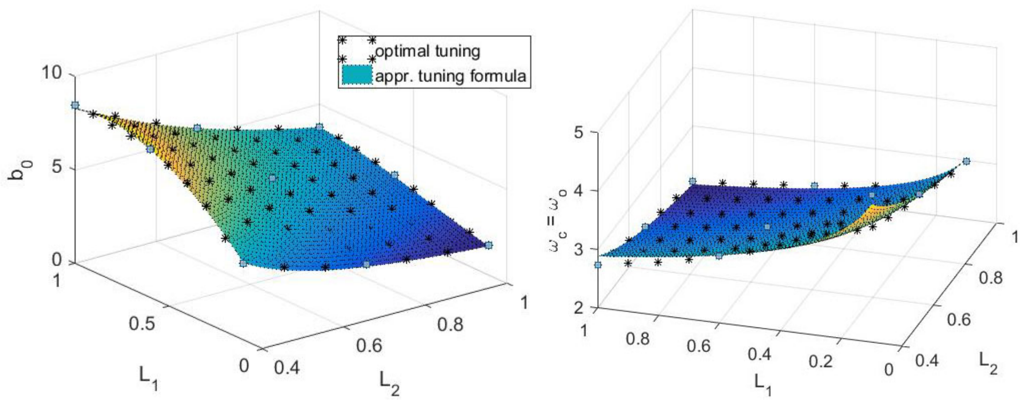


Figure 3: Optimal RADRC2 tunings vs. SOPDT ratios $L_1$ and $L_2$, for GM = 2.5, PM = 60°

Resulting formulas describing RADRC2 tuning rules for SOPDT processes are given by Eqs. (9), (10), where $a = L_1^3 L_2^2$, $b = L_1^2 L_2^2$, $c = L_1^2 L_2$, $d = L_1 L_2^2$, $e = L_1 L_2$. They are normalized with respect to process gain $k$ and its dominant time constant $T_1$.

A3: RADRC2 tuning rule for SOPDT process, GM = 2.5, PM = 60°, disturbance rejection

$$b_0 = \left(\frac{-1.7a+6.5b-4.48c-7.17d+10.52e-1.2L_1+0.9L_2^2+0.08L_2+0.31}{L_2^2}\right)\frac{k}{T_1^2},$$
$$\omega_c = \omega_o = \left(2L_1^{-0.18}L_2^{-0.4}\right)\frac{1}{T_1}. \tag{9}$$

A4: RADRC2 tuning rule for SOPDT process, GM = 2, PM = 45°, disturbance rejection

$$
\begin{aligned}
b_0 &= \left(\frac{-2.2a+7.19b-5.13c-6.1d+8.91e-0.79L_1+0.59L_2^2+0528L_2+0.2}{L_2^2}\right)\frac{k}{T_1^2}, \\
\omega_c &= \omega_o = \left(2.12L_1^{-0.26}L_2^{-0.38}\right)\frac{1}{T_1}.
\end{aligned}
\tag{10}
$$

Readers should note that for each RADRC2 tuning rule A1–A4, optimal tuning is obtained by adjusting $\omega_c = \omega_o$, in contrast to the most popular rule of thumb [6].

Summarizing, if the process has SOPDT dynamics, it can be controlled by RADRC2 tuned based on its FOPDT approximation (A1–A2) or on its real SOPDT dynamics (A3–A4). Additionally, readers should note that if FOPDT process approximation is derived for tuning RADRC2, it can be also applied for tuning RADRC1 by using the rules suggested in [13]. Thus, the question arises, which tuning provides better control performance for SOPDT processes. The answer can be seen in Fig. 4, which shows Integral Absolute Error (IAE) values computed for closed-loop systems with selected SOPDT processes and RADRC1 or RADRC2 controllers tuned to preserve the same GM = 2.5 and

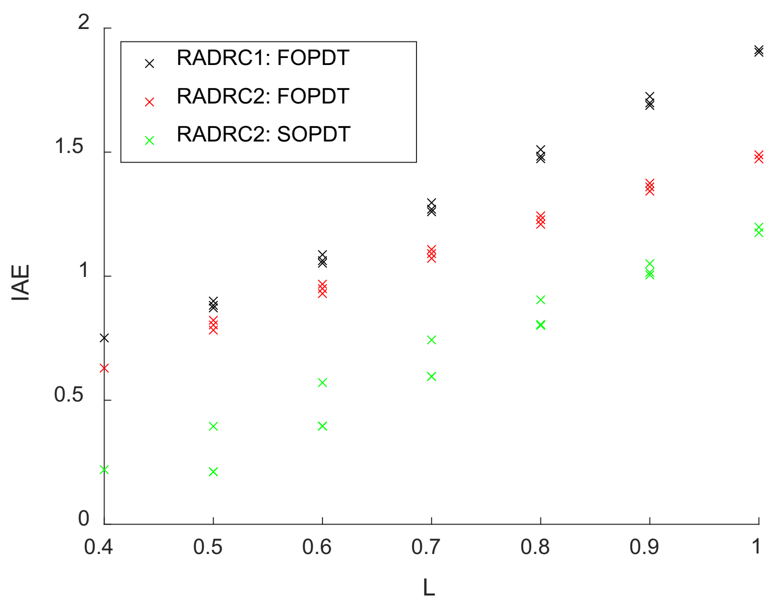


Figure 4: Integral Absolute Error (IAE) for the selected SOPDT processes and RADRC1/RADRC2 controllers, tuned based on FOPDT approximation or SOPDT dynamics for GM = 2.5, PM = 60°

PM = 60°. Results were obtained by simulation using three sets of SOPDT processes parameters: (a) $T_1 = 0.96$, $T_2 = 0.32$, $T_0 \in (0.1, 0.8)$, (b) $T_1 = 0.84$, $T_2 = 0.54$, $T_0 \in (0.1, 0.6)$, (c) $T_1 = 0.78$, $T_2 = 0.6$, $T_0 \in (0.1, 0.5)$. They were selected to cover the range of $L \in (0.4, 1)$ for FOPDT approximation. RADRC1 was tuned by the rule B1 [13] while RADRC2 by the rules A1 and A3.

Results shown in Fig. 4 confirm that for each considered process, RADRC2 tuned by A3 based on SOPDT dynamics provides the best control performance regardless of value of $L$ for its FOPDT approximation. Then, deterioration in control performance is observed when RADRC2 is applied and tuned by A1 based on FOPDT approximation of the real SOPDT process dynamics. This deterioration is relatively large for processes with less significant delay time and it decreases with increment of $L$. Finally, as it was expected, RADRC1 tuned by B1 [13] and based on the same FOPDT approximation of SOPDT process provides the highest values of IAE. Thus, it can be concluded that if the process has SOPDT dynamics, it is always advised to control it by RADRC2 tuned by A3 or A4 (depending on required robustness) based on real SOPDT dynamics. However, this conclusion is based on unrealistic assumption that the real process has SOPDT dynamics and that its parameters are perfectly known. In the next section, more realistic cases are considered.

## 5. Simulation validation

In practice, process dynamics can be more complex than SOPDT and then, FOPDT or SOPDT model can be derived only as a more or less accurate approximation of process dynamics. Thus, it is reasonable to investigate how suggested tuning rules work for such processes. For this purpose, benchmark processes P1–P12 have been selected and presented in Appendix and numerous tests have been done to assess practical applicability of the suggested RADRC2 tuning rules.

First, tuning rules were tested in terms of deviations from active boundary GM/PM assumed for each tuning method. These deviations result from inaccuracy of applied FOPDT or SOPDT approximation of process dynamics and they are shown in Fig. 5. Positive deviation shows the case when robustness is improved at the cost of more conservative tuning. Negative value denotes breaking assumed GM/PM and consequently more aggressive tuning at the price of lower robustness.

Fig. 5 shows that assumed GM is preserved for almost all processes except P8 and A3 tuning method, where very small negative deviation appears. For all processes, RADRC2 tuned based on FOPDT approximation also provides significantly larger GM comparing to RADRC2 tuning based on SOPDT model. It can be also seen that for some processes, PM is broken but ΔPM does not exceed −3°. Additionally, it is worth noting that for P1 and P2, assumed limitation for $L_2 > 0.4$ is not met but RADRC2-based control system still works properly.

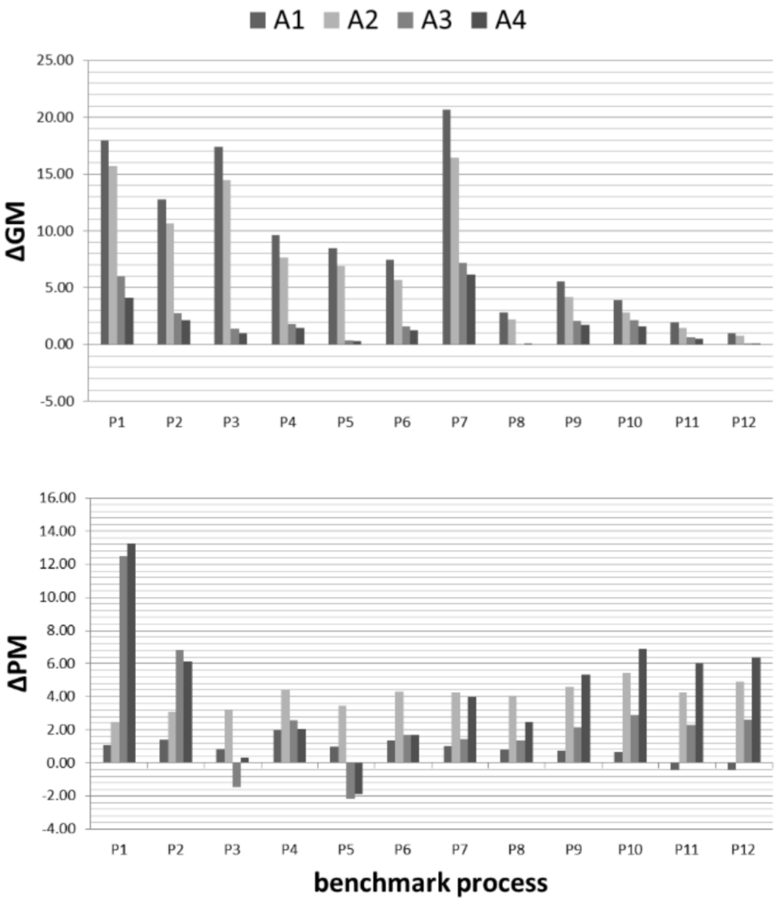


Figure 5: Increments $\Delta$ GM and $\Delta$ PM for benchmark processes tuned based on FOPDT approximation (rules A1–A2) and SOPDT approximation (rules A3–A4)

Performance of RADRC2-based closed systems tuned based on the suggested rules A1–A4 were also compared with conventional PID control for each benchmark process. Three rules of PID tuning were applied: Chien-Hrones-Reswick method with 0% overshoot for load disturbance rejection (CHR) [4], the method proposed by Vilanova [17] and SIMC method [15], which is based on SOPDT process approximation. Results of this qualitative comparison are presented in Fig. 6. Each experiment includes tracking performance in the presence of unitary set point step applied at $t = 0$ and load disturbance rejection in the presence of negative unitary step change of load disturbance applied at the middle of each simulation period.

More quantitative comparison can be made using popular quality indices frequently used for assessing control performance: IAE value, settling time $Y_{\text{set}}$

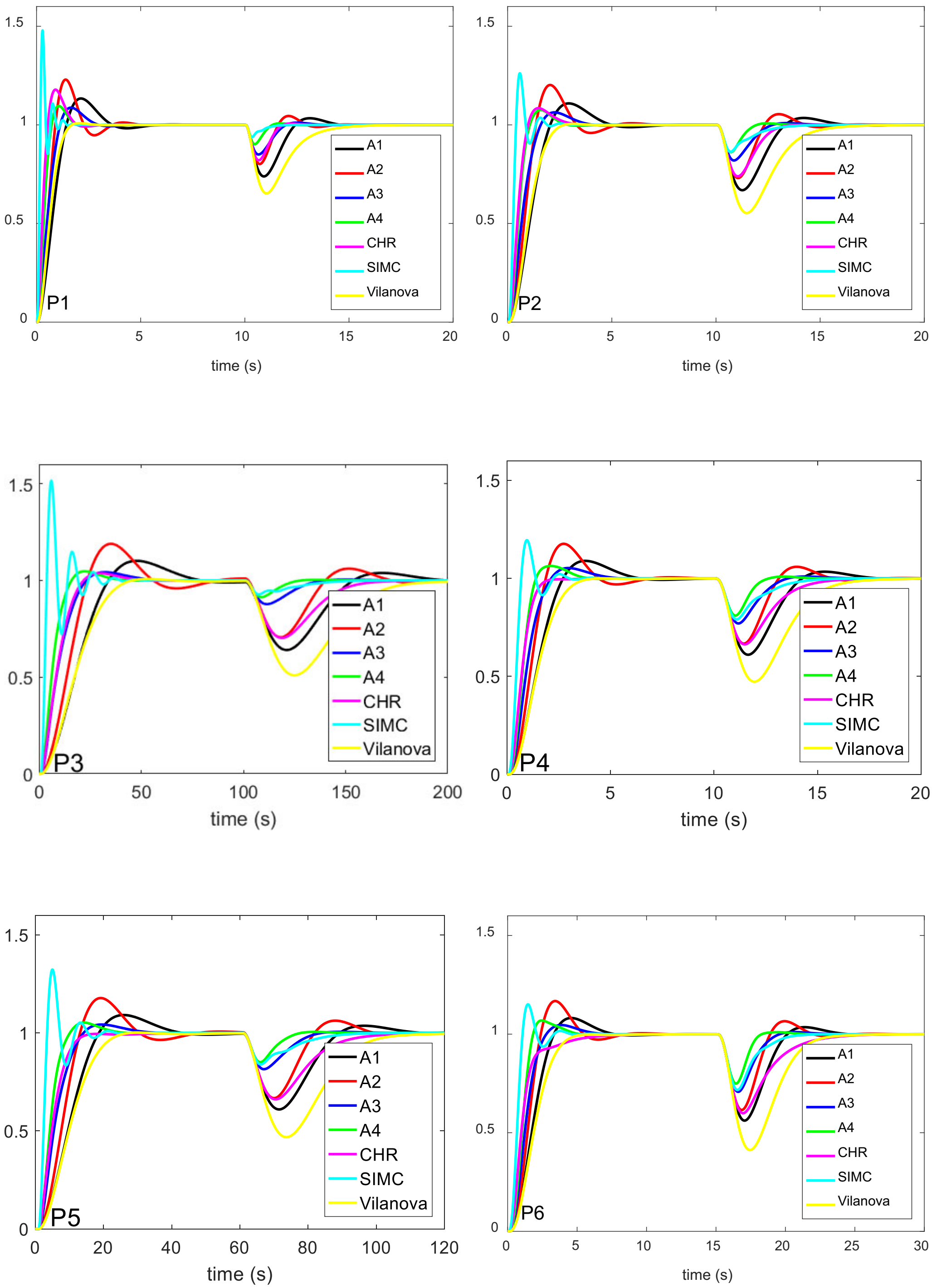
P1
A1
A2
A3
A4
CHR
SIMC
Vilanova
time (s)
P2
A1
A2
A3
A4
CHR
SIMC
Vilanova
time (s)
P3
A1
A2
A3
A4
CHR
SIMC
Vilanova
time (s)
P4
A1
A2
A3
A4
CHR
SIMC
Vilanova
time (s)
P5
A1
A2
A3
A4
CHR
SIMC
Vilanova
time (s)
P6
A1
A2
A3
A4
CHR
SIMC
Vilanova
time (s)

Figure 6.

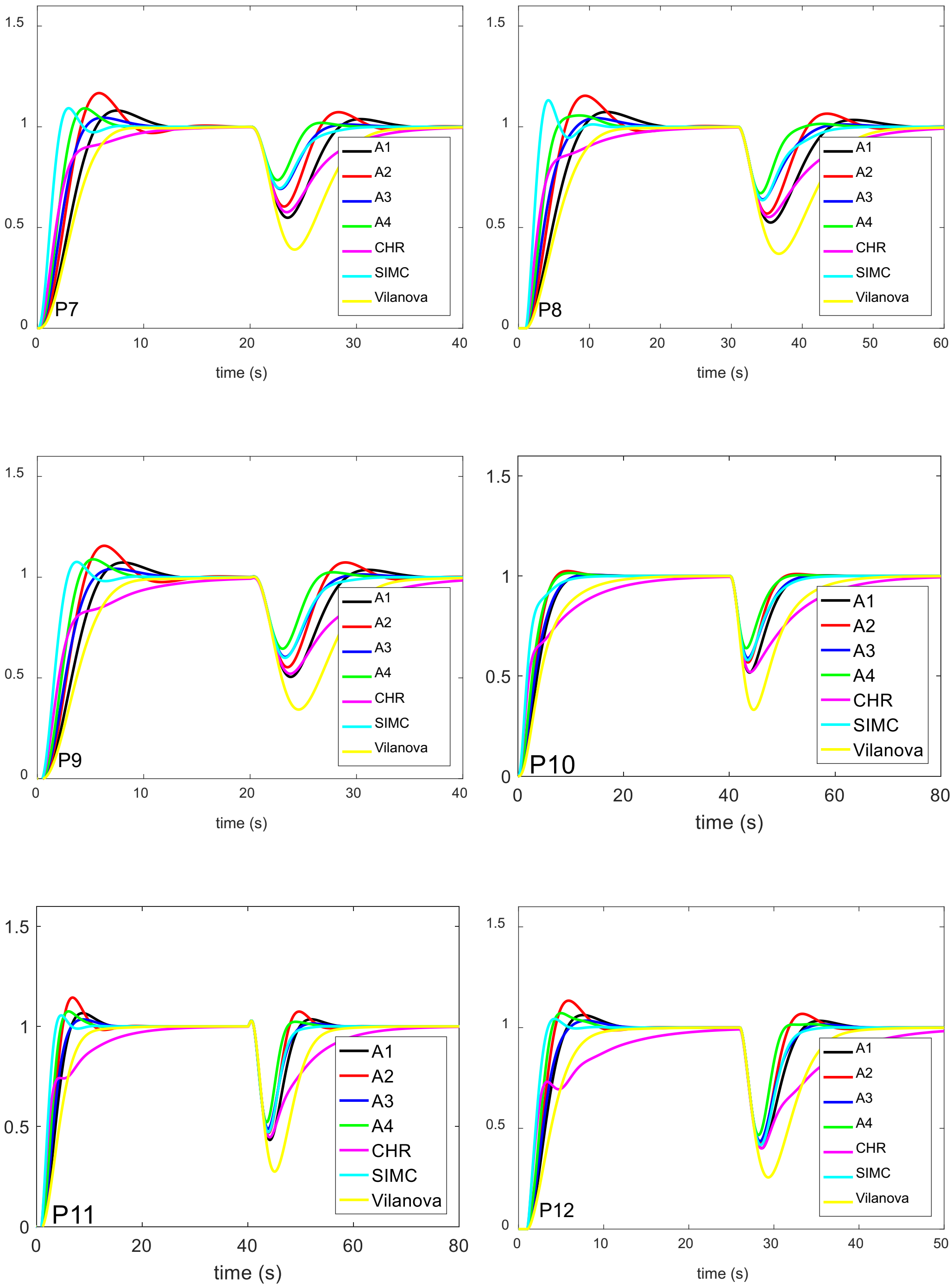


Figure 6: Closed-loop performance for different controllers and different tuning methods, for benchmark processes P1–P12

and maximum overshoot $Y_{\max}$. Each index was separately computed for tracking (SP subscript) and for disturbance rejection (DR subscript). Table 1 shows mean values of these indices for each controller and each tuning method, unified according to specific dynamics of each process and then averaged by all benchmark processes P1–P12. Due to normalization to the minimum value, the best control performance corresponds to a unitary value. The only exception is tracking ($\overline{Y}_{\max\ \mathrm{SP}}$) where there was no necessity of any normalization and results should be considered as mean percentage maximum overshoot. Additionally, in Table 1, mean values of PM and GM are shown jointly with mean sensitivity function value $M_S = |S(j\omega)|$ where $S(j\omega) = 1/(1 + K(j\omega))$ and $K(j\omega)$ denotes open-loop transfer function.

Table 1: Benchmark dynamical processes

| Quality index | Applied controller and its tuning method | | | | | | |
|---|---|---|---|---|---|---|---|
| | RADRC2 | | | | PID | | |
| | A1 | A2 | A3 | A4 | CHR | SIMC | Vil |
| $\overline{\mathrm{IAE}}_{\mathrm{SP}}$ | 2.52 | 2.21 | 1.77 | 1.41 | 1.74 | **1** | 2.51 |
| $\overline{T}_{\mathrm{set\,SP}}$ | 2.27 | 2.37 | 1.81 | 1.4 | 2.23 | **1.1** | 1.68 |
| $\overline{Y}_{\max\ \mathrm{SP}}$ | 8 | 16 | 4 | 7 | 2 | 19 | **0** |
| $\overline{\mathrm{IAE}}_{\mathrm{DR}}$ | 4.09 | 2.87 | 1.76 | **1.06** | 3.67 | 1.43 | 6.95 |
| $\overline{T}_{\mathrm{set\,DR}}$ | 2.58 | 2.07 | 1.34 | **1.03** | 2.64 | 1.46 | 2.76 |
| $\overline{Y}_{\max\ \mathrm{DR}}$ | 2.18 | 1.85 | 1.31 | **1.07** | 1.87 | 1.09 | 2.93 |
| $\overline{\mathrm{PM}}$ | 60.83 | 49.05 | 62.73 | 49.38 | 78.32 | 51.47 | **69.33** |
| $\overline{\mathrm{GM}}$ | **11.63** | 9.41 | 4.66 | 3.69 | 7.64 | 3.19 | 8.69 |
| $\overline{M}_S$ | **1.27** | 1.48 | 1.54 | 1.79 | 1.35 | 1.95 | 1.34 |

For tracking performance, PID tuned by SIMC provides the best $\overline{\mathrm{IAE}}_{\mathrm{SP}}$ and $\overline{T}_{\mathrm{set\,SP}}$ values but at the price of high 20% overshoot shown by $\overline{Y}_{\max\ \mathrm{SP}}$. For disturbance rejection, RADRC2 tuned by A4 provides the rm best $\overline{IAE}_{\mathrm{SP}}$ and $\overline{T}_{\mathrm{set\,SP}}$, this time with very small overshoot of 7%. At the same time, RADRC2 tuned by A1 provides very good robustness shown by the indices $\overline{\mathrm{PM}}$, $\overline{\mathrm{GM}}$ and $\overline{M}_S$.

Conclusion is that tuning of RADRC2 based on SOPDT process approximation provides better control performance. PID controller provides better tracking but RADRC2 ensures better disturbance rejection, which is very important in process automation. Thus, results shown in Table I confirm that RADRC2 tuned by the suggested rules can be an alternative for conventional PID controller.

## 6. Practical validation

Practical validation is based on the setup designed as a serial connection of three pneumatic tanks shown in Fig. 7. Supplying pressure $p_s$ is adjusted within the range 0–5 bar by proportional valve MPPES-3-1 from Festo. Each tank has different volume denoted respectively as $V_1 = 5L$, $V_2 = 2L$ and $V_3 = 0.75L$. Pressures in tanks are respectively denoted as $p_1$, $p_2$, $p_3$ bar and they are measurable on-line. There is a single outlet from the last tank and air flows out through swiching pneumatic resistance $R_{pout}$. Switching takes place automatically between two different pneumatic valves representing different pneumatic resistances. On-line measurement data is collected by dedicated SCADA system implemented in Zenon from COPA-DATA. All considered controllers were implemented in industrial PLC – Siemens S7-1500.

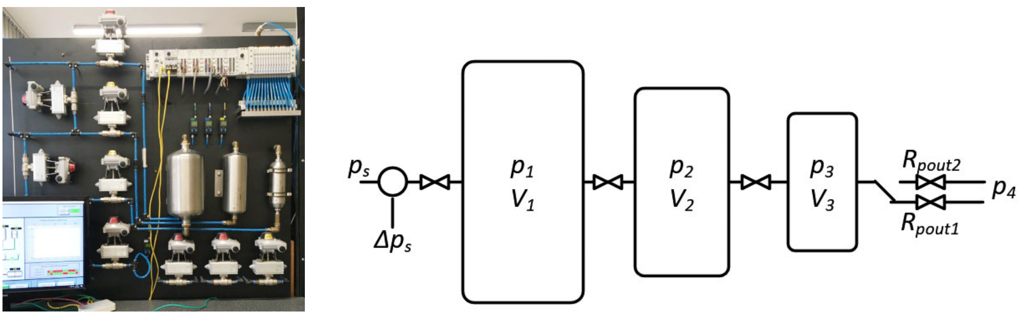


Figure 7: Laboratory pneumatic setup – overview and simplified diagram

During experiments, problem of stabilization of process output $Y = p_3$ at the setpoint $SP$ was considered as the control goal. Controller output was the supplying pressure $u = p_s$. Experiments were designed to validate both tracking and disturbance rejection. For the latter, one possibility is to apply load disturbance $\Delta p_s$ (bar) added directly to controller output. This disturbance influences process output without any changes in its dynamics. The other disturbance is switching between two different pneumatic resistances $R_{pout}$ at the outlet from the last tank. In this case, apart from disturbing process output, switching significantly changes dynamics of the process due to its nonlinear nature [11].

For tuning of considered controllers, process step response was approximated by FOPDT and SOPDT models. For the chosen operating point ($p_s = 2.5$ at inlet and corresponding $p_3 = 1.0$, with disturbing $R_{pout1}$ at outlet and $\Delta p_s = 0$), FOPDT parameters are: $k = 0.65$ (–), $T = 12.54$ (s), $T_0 = 4.25$ (s) and SOPDT parameters are: $k = 0.65$ (–), $T_1 = 10.97$ (s), $T_2 = 4.13$ (s), $T_0 = 1.29$ (s). Based on these values, RADRC2 was tuned by the suggested rules A1-A4. For comparison, conventional PID controller was applied and tuned by SIMC and CHR.

For better clarity, validation was divided into two stages. The first stage was based on scenario including step changes of setpoint from 1 bar to 1.4 bar at $t = 30$ s. Then, setpoint was changed again to 1 bar in $t = 110$ s and at $t = 190$ s, load disturbance $\Delta p_s = 1.5$ was applied to the system. $\Delta p_s = 0$ was set back at $t = 250$ s. At this stage, outlet pneumatic resistance $R_{pout}$ was not changed so dynamical properties of the process remain unaffected over whole experiment. Results are shown in Fig. 8.

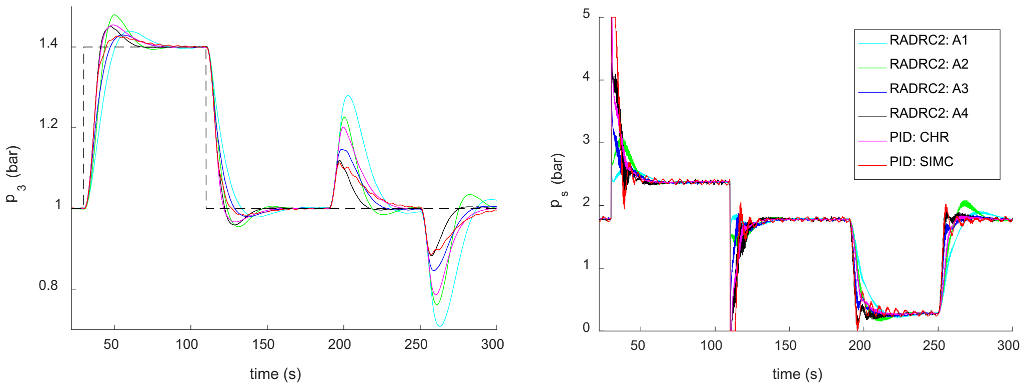


Figure 8: Practical validation for the pneumatic setup, stage one

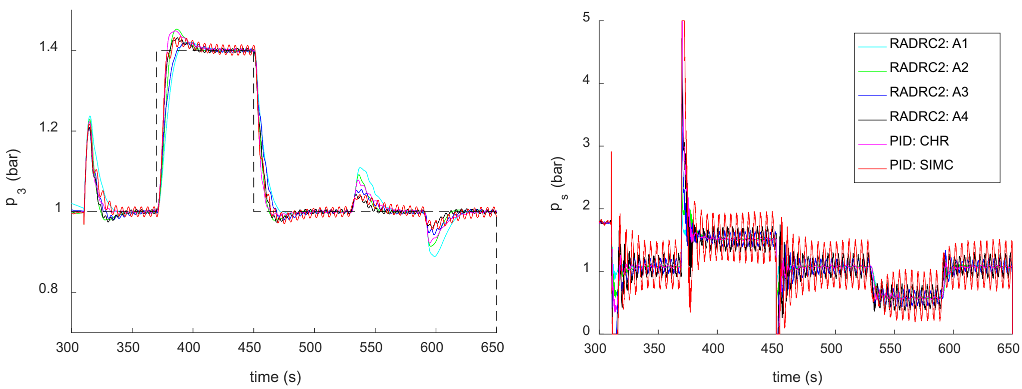


Figure 9: Practical validation for the pneumatic setup, stage two

The second stage of validation shows behaviour of the system after pneumatic resistance $R_{pout}$ has been switched at $t = 310$ s. The rest of experiment has the same scenario as at the first stage shown in Fig. 8 except load disturbance $\Delta p_s = 0.5$, applied due to limited performance of air supply system. Note that after canging value of $R_{pout}$, dynamics of the process changed significantly due to its nonlinearity. However, this change was not considered in tuning because no retuning was applied to any controller comparing to the first stage of validation.

Results show that RADRC2 tuned by A4 provides the best control performance. PID controller tuned by SIMC and RADRC2 tuned by A3 provide comparable control performance. For PID tuned by SIMC, significant oscillations appear at process output. At the same time, RADRC2 tuned by A1–A4 methods provides significantly smoother variations of manipulating signal. Readers should note that even if these variations are filtered by process dynamics, they have a very negative impact on service life of actuators and consequently, such behaviour can be a source of frequent actuator faults.

## 7. Conclusions

In the paper, it is confirmed that RADRC2 controller has the potential ability of more efficient process control if it is properly tuned. Based on optimization tool that uses D-partition method, it is shown how to ensure robust RADRC2 tuning that provides minimization of IAE performance index. Robustness is defined by gain and phase margins and optimisation results in ready to use tuning rules based on FOPDT and SOPDT process approximation.

So far, lack of reliable and easy-to-use tuning rules has been the most significant obstacle for increasing use of RADRC2 in industrial control systems. Tuning rules suggested in this paper remove this obstacle and their applicability is confirmed by comprehensive simulation and practical validation. Thus, practitioners who want to implement RADRC2 for control of industrial processes with significant delay time get a useful tool for its tuning.

## Appendix

This section presents examplary benchmark processes [2] used for validation. Their dynamics is obtained from the following transfer functions:

$$G1(s) = \frac{1}{(1+s)^{\gamma}}, \tag{11}$$

$$G2(s) = \frac{1}{(1+s)(1+\gamma s)\left(1+\gamma^2 s\right)\left(1+\gamma^3 s\right)}, \tag{12}$$

$$G3(s) = \frac{1}{(1+\gamma s)^2} e^{-s}, \tag{13}$$

$$G4(s) = \frac{1-\gamma s}{(1+s)^3}, \tag{14}$$

by adjustment of parameter $\gamma$, as it is shown in Table 2. This table also shows FOPDT and SOPDT approximations of each process obtained by fminsearch()

function in MATLAB environment. Processes are arranged with respect to the value of relative delay time $L = T_0/T$ parameter.

Table 2: Benchmark dynamical processes

| Process | Transfer function | Approximation | | | | | |
|---|---|---|---|---|---|---|---|
| | | FOPDT | | | SOPDT | | |
| | | T | T0 | L | T1 | T2 | T0 |
| P1 | G2, $\gamma = 0.2$ | 1.01 | 0.25 | 0.25 | 1 | 0.20 | 0.05 |
| P2 | G2, $\gamma = 0.3$ | 1.04 | 0.40 | 0.39 | 1 | 0.31 | 0.11 |
| P3 | G3, $\gamma = 10$ | 14.58 | 7.07 | 0.48 | 10 | 10 | 1 |
| P4 | G2, $\gamma = 0.4$ | 1.09 | 0.58 | 0.53 | 0.99 | 0.45 | 0.19 |
| P5 | G3, $\gamma = 5$ | 7.28 | 4.05 | 0.56 | 5 | 5 | 1 |
| P6 | G2, $\gamma = 0.5$ | 1.15 | 0.77 | 0.67 | 0.95 | 0.63 | 0.3 |
| P7 | G1, $\gamma = 3$ | 1.78 | 1.33 | 0.75 | 1.24 | 1.24 | 0.56 |
| P8 | G3, $\gamma = 2$ | 2.91 | 2.22 | 0.76 | 2 | 2 | 1 |
| P9 | G4, $\gamma = 0.2$ | 1.78 | 1.53 | 0.86 | 1.23 | 1.23 | 0.77 |
| P10 | G1, $\gamma = 4$ | 2.06 | 2.10 | 1.02 | 1.43 | 1.43 | 1.20 |
| P11 | G4, $\gamma = 0.5$ | 1.76 | 1.82 | 1.04 | 1.22 | 1.22 | 1.07 |
| P12 | G3, $\gamma = 1$ | 1.45 | 1.61 | 1.11 | 1 | 1 | 1 |

## References

[1] J. Ackermann: *The Parameter Space Approach*, Springer, London 2002.

[2] K.J. Åström and T. Hägglund: Benchmark Systems for PID Control, *IFAC Proc.*, **33**(4) (2000), 165–166.

[3] X. Chen, D. Li, Z. Gao, and C. Wang: Tuning method for second-order active disturbance rejection control, *Proc 30th Chinese Control Conf.* (2011), 6322–6327.

[4] K.L. Chien: On the automatic control of generalized passive systems, *Trans ASME*, **74** (1972), 175–185.

[5] Z. Gao, Y. Huang, and J. Han: An alternative paradigm for control system sign, *Proceedings of the IEEE Conference on Decision and Control*, **5** (2001), 4578–4585.

[6] Z. Gao: Scaling and bandwidth-parameterization based controller tuning, *Proceedings of the 2003 American Control Conference*, **6** (2003), 4989–4996.

[7] G. Herbst: Practical Active Disturbance Rejection Control: Bumpless Transfer, Rate Limitation, and Incremental Algorithm, *IEEE Transactions on Industrial Electronics*, **63**(3), (2016), 1754–1762.

[8] Y. Huang and W. Xue: Active disturbance rejection control: Methodology and theoretical analysis, *ISA Transactions*, **53**(4), (2014), 963–976.

[9] R. Madoński and P. Herman: Survey on methods of increasing the efficiency of extended state disturbance observers. *ISA Transactions*, **56** (2015) 18–27.

[10] R. Madonski, M. Nowicki, and P. Herman: Application of active disturbance rejection controller to water supply system, *Proceedings of the 33rd Chinese Control Conference* (2014), 4401–4405.

[11] P. Nowak and J. Czeczot: Practical verification of active disturbance rejection controller for the pneumatic setup, *22nd International Conference on Methods and Models in Automation and Robotics (MMAR)*, (2017), pp. 19–24.

[12] P. Nowak, K. Stebel, T. Klopot, J. Czeczot, M. Fratczak and P. Laszczyk: Flexible function block for industrial applications of active disturbance rejection controller, *Archives of Control Science*, **28**(3), (2018), 349–400.

[13] P. Nowak, J. Czeczot, and T. Klopot: Robust tuning of a first order reduced Active Disturbance Rejection Controller, *Control Engineering Practice*, **74** (2018), 44–57.

[14] D. Siljak: Generalization of the parameter plane method, *IEEE Transactions on Automatic Control*, **11**(1), (1966), 63–70.

[15] S. Skogestad and C. Grimholt: The SIMC method for smooth PID controller tuning. PID Control in the Third Millennium, *Advances in Industrial Control* (2012) 147–175.

[16] L. Sun, D. Li, K. Hu, K.Y. Lee, and F. Pan: On Tuning and Practical Implementation of Active Disturbance Rejection Controller: A Case Study from a Regenerative Heater in a 1000 MW Power Plant, *Industrial and Engineering Chemistry Research*, **55**(23), (2016), 6686–6695.

[17] R. Vilanova: PID controller tuning rules for robust step response of first-order-plus-dead-time models, *2006 American Control Conference* (2006), 256–261.

[18] Y.J. Wang: Graphical computation of gain and phase margin specifications-oriented robust PID controllers for uncertain systems with time-varying delay, *Journal of Process Control*, **21**(4), (2011), 475–488.

[19] S. Xingling and W. Honglun: Back-stepping active disturbance rejection control design for integrated missile guidance and control system via reduced-order ESO, *Isa Transactions*, **57** (2015), 10–22.

[20] R.Yang, M. Sun, and Z. Chen: Graphical design of linear active disturbance rejection controller for uncertain first-order-plus-dead-time plant, *Proceedings of 2011 International Conference on Modelling, Identification and Control* (2011), 371–375.

[21] B. Zhang, W. Tan, and J. Li: Tuning of linear active disturbance rejection controller with robustness specification, *ISA Transactions*, **85** (2018), 237–246.

[22] Q. Zheng, L.Q. Gao, and Z. Gao: On stability analysis of active disturbance rejection control for nonlinear time-varying plants with unknown dynamics, *IEEE Conference on Decision and Control* (2007), 3501–3506.